



## Letter

Magnetic structure of  $\text{ErCu}_2\text{Ge}_2$ B. Penc<sup>a</sup>, S. Baran<sup>a,\*</sup>, D. Kaczorowski<sup>b</sup>, A. Hoser<sup>c</sup>, A. Szytuła<sup>a</sup><sup>a</sup> M. Smoluchowski Institute of Physics, Jagiellonian University, Reymonta 4, PL-30 059 Kraków, Poland<sup>b</sup> Institute of Low Temperature and Structure Research, Polish Academy of Sciences, P.O. Box 1410, PL-50 950 Wrocław, Poland<sup>c</sup> Helmholtz-Zentrum Berlin, Glienicker Str. 100, D-14 109 Berlin, Germany

## ARTICLE INFO

## Article history:

Received 2 April 2010

Received in revised form 12 April 2010

Accepted 25 April 2010

Available online 10 May 2010

## PACS:

61.12.–q

75.25.+z

75.50.Ee

## Keywords:

Magnetically ordered material

Rare earth intermetallics

Specific heat

Neutron diffraction

## ABSTRACT

The compound  $\text{ErCu}_2\text{Ge}_2$  which crystallizes in the tetragonal  $\text{ThCr}_2\text{Si}_2$ -type crystal structure orders antiferromagnetically at low temperatures. At 1.4 K, the Er magnetic moments are arranged in a commensurate structure described by the propagation vector  $\vec{k} = [1/2, 0, 1/2]$ . The magnetic moment is equal to  $6.80(7) \mu_B$  and forms an angle of  $27^\circ$  with the  $c$ -axis. At  $T_i = 2.6$  K an additional incommensurate magnetic structure appears and at higher temperatures both structures coexist and concurrently disappear at  $T_N = 3.1$  K. The magnetic phase transitions at  $T_i$  and  $T_N$  clearly manifest themselves in the heat capacity and thermal expansion data of the compound.

© 2010 Elsevier B.V. All rights reserved.

## 1. Introduction

The ternary germanides  $\text{RCu}_2\text{Ge}_2$ , where R is a heavy lanthanide atom, crystallize in the body-centered tetragonal structure of the  $\text{ThCr}_2\text{Si}_2$ -type with the space group  $I4/mmm$  [1,2]. The R, Cu and Ge atoms occupy the positions 2(a), 4(d) and 4(e), respectively. The main characteristic feature of the crystal structure is the presence of monoatomic layers perpendicular to the  $c$ -axis, alternating in the sequence R–Cu–Ge–Cu–R. Early magnetic studies [2] indicated that the Gd-, Tb-, Dy- and Ho-based compounds order antiferromagnetically below the Néel temperatures  $T_N = 12, 15, 8$  and  $6.4$  K, respectively, whereas the Er- and Tm-based compounds do not show any magnetic ordering down to  $4.2$  K [2]. Subsequent neutron diffraction measurements revealed commensurate antiferromagnetic order with the same propagation vector  $\vec{k} = [1/2, 0, 1/2]$  in  $\text{TbCu}_2\text{Ge}_2$ ,  $\text{HoCu}_2\text{Ge}_2$  [3],  $\text{DyCu}_2\text{Ge}_2$  [4,5] and  $\text{ErCu}_2\text{Ge}_2$  [6]. For the two former compounds this magnetic structure was claimed to be stable from  $4.2$  K up to the respective  $T_N$  [3,4], however more recent DC susceptibility and magnetization measurements on a single crystal of  $\text{TbCu}_2\text{Ge}_2$  [7,8] clearly showed two magnetic transitions at  $T_N = 12.3$  K and  $T_i = 9.6$  K, the latter being a change in

the magnetic moments arrangement. The occurrence of additional magnetic phase transition in the antiferromagnetically ordered state is a common feature in the isostructural silicides  $\text{RCu}_2\text{Si}_2$  [9,10]. For example, for  $\text{ErCu}_2\text{Si}_2$  the neutron diffraction data indicated a change in the magnetic structure from a collinear one below  $1$  K to a modulated structure near  $T_N = 1.5$  K [11].

By means of bulk magnetic and electrical transport measurements we recently established that  $\text{ErCu}_2\text{Ge}_2$  orders antiferromagnetically below the Néel temperature equal to  $3.1$  K [12]. The main aim of the present work was to prove by neutron diffraction if the magnetic structure previously observed at  $1.9$  K [6] is stable up to  $T_N$ .

## 2. Experimental details

Polycrystalline sample of  $\text{ErCu}_2\text{Ge}_2$  was prepared by arc melting the constituents (Er: 99.9 wt%; Cu: 99.9 wt%; Ge: 99.9 wt%) under titanium-gettered argon atmosphere. The melted ingot was subsequently annealed in an evacuated silica tube at  $870$  K for one week. Quality of the product was checked by X-ray powder diffraction at room temperature using the Philips PW-3710 X'PERT diffractometer ( $\text{CuK}_\alpha$  radiation). The neutron powder diffraction patterns were collected at temperatures ranging from  $1.4$  to  $12.0$  K on the E6 diffractometer installed at the BER II reactor (BENS, Helmholtz-Zentrum Berlin). The incident neutron wavelength was  $2.45$  Å. The neutron diffraction data were analyzed using the Rietveld program FullProf [13]. Heat capacity measurements were done in the temperature range  $0.4$ – $5$  K by relaxation method employing a Quantum Design PPMS platform.

\* Corresponding author. Tel.: +48 12 6635686; fax: +48 12 6337086.  
E-mail address: [stanislaw.baran@uj.edu.pl](mailto:stanislaw.baran@uj.edu.pl) (S. Baran).

**Table 1**

Structural parameters of  $\text{ErCu}_2\text{Ge}_2$  refined from the neutron diffraction data taken at 1.4 and 12.0 K, and the corresponding reliability factors.

$T$ [K]	12.0	1.4
$a$ [Å]	4.002(2)	3.9970(8)
$c$ [Å]	10.305(7)	10.2975(40)
$c/a$	2.575(3)	2.576(2)
$V$ [Å <sup>3</sup> ]	165.41(28)	164.51(13)
$z$	0.378(1)	0.378(1)
$R_{\text{Bragg}}$ [%]	7.1	6.7
$R_{\text{profile}}$ [%]	6.2	3.5

### 3. Crystal structure

The X-ray diffraction data collected at room temperature as well as the neutron diffraction data recorded at all measured temperatures unambiguously confirmed that  $\text{ErCu}_2\text{Ge}_2$  crystallizes in a tetragonal unit cell of the  $\text{ThCr}_2\text{Si}_2$ -type. In this crystal structure the atoms are located at the following sites:

2 Er atoms at 2(a) site	0, 0, 0
4 Cu atoms at 4(d) site	$0, \frac{1}{2}, \frac{1}{4}; \frac{1}{2}, 0, \frac{1}{4}$
4 Ge atoms at 4(e) site	$0, 0, z; 0, 0, \bar{z}$
	+body centering translation

The lattice parameters and the free positional parameter  $z$ , determined from the neutron data collected at 1.4 and 12.0 K are listed in Table 1. The obtained values are in good agreement with the literature data [6].

### 4. Magnetic structure

The differential neutron diffraction patterns obtained at 1.4 and 2.7 K are displayed in Fig. 1. In agreement with Ref. [6], at 1.4 K, all the additional Bragg peaks of magnetic origin can be well described by the propagation vector  $\vec{k} = [1/2, 0, 1/2]$ , which corresponds to the magnetic structure with ferromagnetic (1 0 1) planes stacked antiferromagnetically. The magnetic moment equal  $6.80(7) \mu_B$  forms an angle  $\theta = 27^\circ$  with the  $c$ -axis ( $R_{\text{magn}} = 9.4\%$ ). The magnetic moment value is notably smaller than the free  $\text{Er}^{3+}$  ion value ( $9 \mu_B$ ), yet it should be noted that the experiment was performed at  $T = 0.47T_N$ .

The above-described type of magnetic order is stable up to 2.5 K. As it is apparent from Fig. 1, the pattern recorded at 2.7 K contains several other magnetic reflections besides those observed at lower temperatures. These additional Bragg peaks can be accounted for by considering the incommensurate wave vector  $\vec{k} = [k_x, 0, k_z]$  where  $k_x = 0.5514(7)$  and  $k_z = 0.5375(37)$  at  $T = 2.7$  K. Analyses of the neutron diffraction pattern indicated the coexistence of two magnetic structures: one collinear, with the magnetic moment equal  $3.11(5) \mu_B$ , and the other modulated, with the amplitude  $\mu = 5.64(7) \mu_B$  ( $R_{\text{magn}} = 15.1\%$ ). Similar coexistence of the two propagation vectors was found for the temperatures 2.9 and 3.1 K. The  $k_x$  component is almost unaffected by a change of temperature while the  $k_z$  component slightly decreases with increasing temperature. With further rising the temperature both magnetic contributions to the neutron diffraction pattern consecutively decrease and both are entirely absent at 3.2 K.

The temperature variations of the magnetic moment in the commensurate structure as well as of the refined values of the modulated magnetic moment  $\mu_m$  are shown in the inset in Fig. 1. The latter quantity reaches its maximum of  $5.64(7) \mu_B$  at 2.7 K, i.e. in the temperature region where the magnetic moment associated with the commensurate structure starts to decrease rapidly. The two phase transitions are evident in the temperature dependence of the specific heat of the compound studied—the observed maxima are at  $2.54(9)$  and  $3.04(6)$  K (cf. Fig. 2).

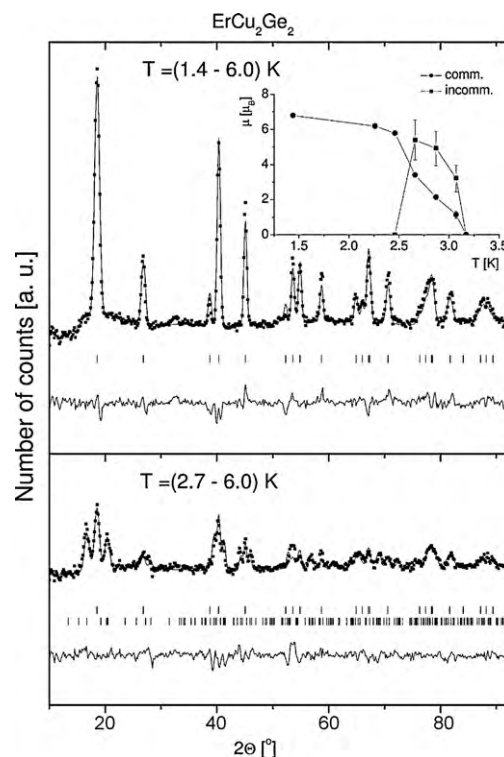


**Fig. 1.** Differential neutron diffraction patterns of  $\text{ErCu}_2\text{Ge}_2$  together with Rietveld fit and difference plot. The patterns were constructed as a difference between experimental patterns collected at 1.4 and 6.0 K (top), and 2.7 and 6.0 K (bottom). The vertical ticks indicate the positions of the magnetic reflections for the commensurate structure (upper row) and the incommensurate structure (lower row). The inset presents the temperature variations of the commensurate magnetic moment (circles) and the magnitude of modulation of the incommensurate magnetic moment (squares) in  $\text{ErCu}_2\text{Ge}_2$ .

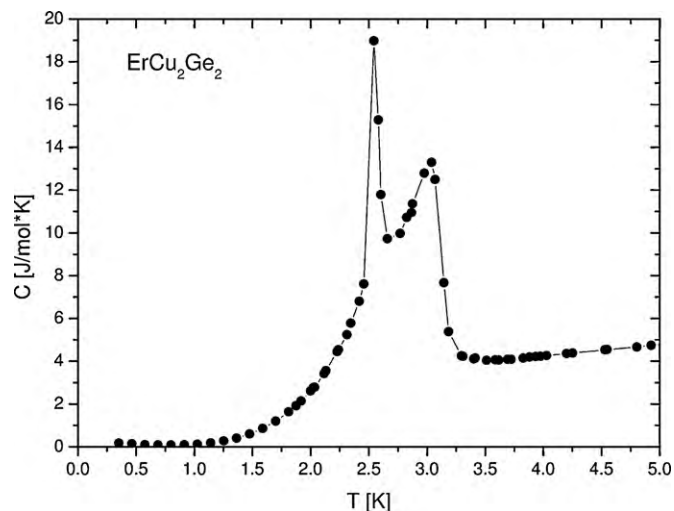


**Fig. 2.** Temperature variation of the low-temperature specific heat of  $\text{ErCu}_2\text{Ge}_2$ .

### 5. Conclusions

The neutron diffraction data corroborate that  $\text{ErCu}_2\text{Ge}_2$  is antiferromagnetic at low temperatures. In the temperature range 1.4–2.5 K, the magnetic order is described by a wave vector  $\vec{k} = [1/2, 0, 1/2]$ , typical for the  $\text{RCu}_2\text{X}_2$  ( $X = \text{Si}, \text{Ge}$ ) compounds with R being a heavy rare earth element [14]. Above  $T = 2.5$  K, an incommensurate propagation vector  $\vec{k} = [k_x, 0, k_z]$  develops, yielding a coexistence of two magnetic structures. Similar changes in the

**Table 2**

Comparison of the key magnetic parameters of  $\text{ErCu}_2\text{Ge}_2$  and  $\text{ErCu}_2\text{Si}_2$ .  $T_N$  denotes Néel temperature,  $T_t$ : additional transition temperature,  $\mu_c$ : collinear component of the magnetic moment,  $\mu_m$ : modulated component of the magnetic moment.

	$T_N$ [K]	$T_t$ [K]	$k_x$	$\mu_c$ [ $\mu_B$ ]	$\mu_m$ [ $\mu_B$ ]	Ref.
$\text{ErCu}_2\text{Ge}_2$	3.1	2.6	0.113(2)	6.80(7) (at 1.4 K)	5.64(7) (at 2.7 K)	This work
$\text{ErCu}_2\text{Si}_2$	1.5	1.0	0.074(1)	4.94(15) (at 0.47 K)	4.61(17) (at 1.2 K)	[11]

magnetic structure were observed in other rare earth intermetallics [15]. In particular, the coexistence of the commensurate and incommensurate propagation vectors over a range in temperature, and the commensurate spin arrangement being the ground state have recently been established for the isostructural silicide  $\text{ErCu}_2\text{Si}_2$  [11]. As may be inferred from Table 2, the phase transitions in the latter compound occur at lower temperatures than in  $\text{ErCu}_2\text{Ge}_2$ . Also the value of  $k_x$  is smaller in the silicide. These differences likely reflect subtle changes in the interplay between magnetic exchange interactions and crystal field effect upon replacement of Si by Ge in the nearest neighbours coordination sphere of the Er atoms.

The experimental value of the Néel temperature in  $\text{ErCu}_2\text{Ge}_2$  ( $T_N = 3.1$  K) is much larger than that calculated on the basis of the de Gennes formula ( $T_N = 1.97$  K, derived by scaling from  $T_N = 12$  K known for  $\text{GdCu}_2\text{Ge}_2$ ). This discrepancy arises due to influence of crystalline electric field (CEF) interactions. Another manifestation of the CEF effect is seen in relatively small values of the magnetic moments determined from the neutron diffraction data. Apparently, the moments are governed by reduction of  $\langle J_2 \rangle$  value related to the CEF ground state [14].

The CEF Hamiltonian relevant for  $\text{ErCu}_2\text{Ge}_2$  describes the influence of CEF potential of  $D_{4h}$  tetragonal symmetry on a  $J = 15/2$  ground multiplet of the  $\text{Er}^{3+}$  ion. The Hamiltonian takes the form  $H_{\text{CEF}} = B_2^0 O_2^0 + B_4^0 O_4^0 + B_4^4 O_4^4 + B_6^0 O_6^0 + B_6^4 O_6^4$ , where  $O_l^m$ 's are the Stevens equivalent operators expressed by the angular momenta  $J_x$ ,  $J_y$  and  $J_z$ , while  $B_l^m$ 's are the CEF parameters. In such a crystal field the  $^4I_{15/2}$  multiplet of  $\text{Er}^{3+}$  splits onto eight Kramers doublets. In the case of  $\text{ErCu}_2\text{Si}_2$ , the parameter  $B_2^0$  is negative [10] and thus, according to the prediction by Greedan and Rao [16], the magnetic moment should be parallel to the  $c$ -axis. In reality, the magnetic moments in  $\text{ErCu}_2\text{Si}_2$  are canted with respect to the  $c$ -axis [11]. Similar canting is observed in the germanide  $\text{ErCu}_2\text{Ge}_2$ . These experimental findings indicate some influence of the higher  $B_n^m$  parameters in particularly  $B_6^0$  [17]. The similarity between the

magnetic structures of  $\text{ErCu}_2\text{Si}_2$  and  $\text{ErCu}_2\text{Ge}_2$  imply quite similar CEF parameters in both compounds.

### Acknowledgements

This research project has been supported by the European Commission under the 6th Framework Programme through the Key Action: Strengthening the European Research Area, Research Infrastructures (contract no: RII3-CT-2003-505925 (NM13)) and by the National Scientific Network: "Strongly correlated materials: preparation, fundamental research and applications".

### References

- [1] W. Rieger, E. Parthé, Monatshefte für Chemie 100 (1969) 444.
- [2] P.A. Kotsanidis, J.K. Yakinthos, Solid State Commun. 40 (1981) 1041.
- [3] P. Schobinger-Papamantellos, A. Niggli, P.A. Kotsanidis, J.K. Yakinthos, J. Phys. Chem. Solids 45 (1984) 695.
- [4] H. Pinto, M. Melamud, M. Kuznietz, H. Shaked, Phys. Rev. B 31 (1985) 508.
- [5] P.A. Kotsanidis, J.K. Yakinthos, E. Roudaut, Solid State Commun. 50 (1984) 413.
- [6] J.K. Yakinthos, J. Magn. Magn. Mater. 46 (1985) 300.
- [7] C. Song, D. Johnson, D. Wermeille, A.I. Goldman, S.L. Bud'ko, I.R. Fisher, P.C. Canfield, Phys. Rev. B 64 (2001) 224414.
- [8] T. Shigeoka, M. Shiraishi, H. Mitamura, Y. Uwatoko, T. Fujiwara, T. Goto, Physica B 346–347 (2004) 112.
- [9] Y. Takeda, N.D. Dung, Y. Nakano, T. Ishikura, S. Ikeda, T.D. Matsuda, E. Yamamoto, Y. Haga, T. Takeuchi, R. Settai, Y. Ōnuki, J. Phys. Soc. Jpn. 77 (2008) 104710.
- [10] N.D. Dung, Y. Ota, K. Sugiyama, T.D. Matsuda, Y. Haga, K. Kindo, M. Hagiwara, T. Takeuchi, R. Settai, Y. Ōnuki, J. Phys. Soc. Jpn. 78 (2009) 024712.
- [11] S. Baran, Ł. Gondek, A. Szytuła, D. Kaczorowski, A. Pikul, B. Penc, P. Piekarczyk, A. Hoser, S. Gerischer, J. Magn. Magn. Mater. 322 (2010) 12.
- [12] Ł. Gondek, D. Kaczorowski, A. Pikul, A. Szytuła, in press.
- [13] J. Rodríguez-Carvajal, Physica B 192 (1993) 55.
- [14] D. Gignoux, D. Schmitt, in: K.H.J. Buschow (Ed.), Handbook of Magnetic Materials, vol. 10, Elsevier Science B.V., 1997, chapter 2, p. 239 (see p. 371).
- [15] D. Gignoux, D. Schmitt, Phys. Rev. B 48 (1993) 12682.
- [16] J.E. Greedan, V.U.S. Rao, J. Solid State Chem. 6 (1973) 387, 8 (1973) 368.
- [17] P. Schobinger-Papamantellos, K.H.J. Buschow, C. Ritter, L. Keller, J. Magn. Magn. Mater. 264 (2003) 130.